Earthquakes and Structures, *Vol. 9, No. 1 (2015) 145-171*
DOI: http://dx.doi.org/10.12989/eas.2015.9.1.145

Ratio of Torsion (ROT): An index for assessing the global induced torsion in plan irregular buildings

Chrysanthi G. Stathi[a], Nikolaos P. Bakas[b], Nikos D. Lagaros[*] and Manolis Papadrakakis[c]

Institute of Structural Analysis & Antiseismic Research Department of Structural Engineering, School of Civil Engineering, National Technical University, Athens 9, Iroon Polytechniou Str., Zografou Campus GR-157 80, Athens, Greece

(Received July 14, 2014, Revised March 30, 2015, Accepted April 6, 2015)

Abstract. Due to earthquakes, many structures suffered extensive damages that were attributed to the torsional effect caused by mass, stiffness or strength eccentricity. Due to this type of asymmetry torsional moments are generated that are imposed by means of additional shear forces developed at the vertical resisting structural elements of the buildings. Although the torsional effect on the response of reinforced concrete buildings was the subject of extensive research over the last decades, a quantitative index measuring the amplification of the shear forces developed at the vertical resisting elements due to lateral-torsional coupling valid for both elastic and elastoplastic response states is still missing. In this study a reliable index capable of assessing the torsional effect is proposed. The performance of the proposed index is evaluated and its correlation with structural response quantities like displacements, interstorey drift, base torque, shear forces and upper diaphragm's rotation is presented. Torsionally stiff, mass eccentric single-story and multistory structures, subjected to bidirectional excitation, are considered and nonlinear dynamic analyses are performed using natural records selected for three hazard levels. It was found that the proposed index provides reliable prediction of the magnitude of torsional effect for all test examples considered.

Keywords: torsional effect; mass eccentric; torsionally stiff; center of rigidity; nonlinear dynamic analyses

1. Introduction

Asymmetry is introduced into a structural system by its non-symmetric topology of the structural elements or mass distribution. In particular, structural asymmetry results to eccentric structural systems having different loci of the mass and rigidity centers. During dynamic excitation, the resultant of inertia forces acts through the mass center, while the resultant of resisting forces acts through the rigidity center. As a consequence a moment between the two

∗Corresponding author, Assistant Professor, E-mail: nlagaros@central.ntua.gr
[a]Ph.D., E-mail: cstathi@central.ntua.gr
[b]Ph.D., E-mail: nibas@mail.ntua.gr
[c]Professor, E-mail: mpapadra@central.ntua.gr

 ISSN: 2092-7614 (Print), 2092-7622 (Online)

forces is developed, which induces torsional effect coupled with the lateral motion. Even in case of buildings possessing two axes of symmetry, moments arise due to earthquake rotational component (Chopra 1987). A number of studies have been published dealing with the structural response of reinforced concrete (RC) buildings taking into consideration the lateral-torsional coupling (Jeong and Elnashai 2005, Chandler *et al*. 1996, De La Colina 1999, Humar and Kumar 1998). In most structural design codes, the effect of torsion is treated by implementing accidental and static eccentricities together with specific provisions for addressing the design of irregular buildings. Accidental eccentricity is defined as a percentile (e.g., 5%) of the plan view dimension that is perpendicular to the direction of the lateral forces applied. On the other hand the implementation of the static eccentricity is more complicated, since it is defined with reference to the location of the rigidity center whose position, for the case of multistory buildings, is not unique and is load-dependent. It is for this reason that the efficiency of torsional codified provisions has been studied by many researchers (Chandler and Duan 1997, Chopra and Goel 1991).

For the case of single-story systems there is a point on the diaphragm with the following properties: (i) no rotation is induced when a lateral load is applied to it (rigidity center), (ii) or when the resultant of the shear forces is applied to it (shear center), (iii) remains constant when the structure is subjected to torque loading (center of twist). Consequently, these centers are coincident and load-independent for single-story systems. However, for the case of multistory buildings these centers do not coincide and their effect has been the subject of extensive investigation by many researchers in the past. Inconsistent observations have been attributed to the varying model assumptions implemented, while a detailed overview has been presented by Rutenberg (2002). Cheung and Tso (1986) proposed the generalized center of rigidity and twist under linear response, while Tso (1990) compared two approaches in an effort to measure the story torsional moments for multistory buildings. In particular, the torsional moment is calculated using the floor eccentricity in the first approach, and the story eccentricity in the second. Smith and Vezina (1985) defined the story rigidity center of multistory buildings as the point on the story diaphragm where no torsional action is developed from the application of external horizontal load. Riddell and Vasquez (1984) concluded that the centers of rigidity exist only for a special class of multistory buildings. Trombetti and Conte (2005) developed a simplified analysis procedure in order to evaluate the maximum rotational response of single-story linear elastic systems subjected to earthquake excitation. Lagaros *et al.* (2006) proposed a combined topology-sizing optimum design formulation for RC buildings aiming at minimizing the material cost as well as the static and strength eccentricities taking into account both design code and architectural restrictions. While Trombetti *et al*. (2013) proposed a simplified procedure able to evaluate the maximum corner displacement. Bosco *et al*. (2015) evaluated the effectiveness of three nonlinear static methods for the prediction of the dynamic response of in-plan irregular buildings. A detailed state of the art review on earthquake induced torsion in buildings is provided in the recent work by Anagnostopoulos *et al.* (2015).

Research interest extended also to the inelastic response of sinlge-story structures (Stathopoulos and Anagnostopoulos 2003, Peruš and Fajfar 2005, Lucchini *et al.* 2009). De la Llera and Chopra (1995) proposed the base shear and torque surfaces (BST), which represent all combinations of base shear and torque that would lead to structural collapse when applied statically. They also extended this idea to multistory buildings, the so-called story shear and torque (SST) ultimate surface (De La Llera and Chopra 1995). The surface is constructed for each story and depicts all combinations of story shears and torque that when applied statically would lead the story to collapse. The construction of the surface is based on the implementation of a single super-

element (SE) per building story. An SE of a building consists of a single fictitious structural element per story capable of representing its elastic and inelastic properties. Paulay (1997, 1998) proposed the center of resistance and identified the elastoplastic mechanism, aiming at estimating the torsional effects on the seismic response of ductile buildings, classifying them either as torsionally unrestrained or as torsionally restrained based on the degree of control over the inelastic twist. Makarios and Anastassiadis (1998a, 1998b) estimated the position of the optimum torsion axis for multistory buildings through a parametric analysis of frame-wall systems. Myslimaj and Tso (2002, 2005) proved that the torsional effect can be reduced for asymmetric wall-type systems by locating the center of strength and the center of rigidity on the opposite sides of the center of mass. Marino and Rossi (2004) proposed mathematical formulations aiming to define more accurately the location of the optimum torsion axis. Makarios (2008) has also computed the torsional stiffness radius of a tall multistory system implementing continuous modeling via a mathematical formulation. Anagnostopoulos *et al.* (2010) indicated the inadequacies of simplified single-story, shear-beam type systems for predicting the inelastic response of asymmetric, multistory framed buildings, subjected to torsion due to earthquake motions and for deriving general conclusions concerning the torsional provisions of the design codes. A new design procedure was proposed by Kyrkos and Anagnostopoulos (2011a, b) containing a modification, which leads to a more uniform distribution of ductility demands in the elements between stiff and flexible edges of the buildings eliminating simultaneously the misuse of material and the possibility of overload of the "flexible" edge members. Rossi *et al.* (2013) also developed a new method for estimating the static eccentricity and the uncoupled torsional to lateral frequency ratio. Karimiyan *et al*. (2014) investigate the progressive collapse mechanism of regular and irregular six-story buildings exhibiting mass asymmetry. Georgoussis (2014) presented a modified procedure for assessing the seismic response of elastic non-proportionate multistory buildings.

In the present study an efficient assessment index of the torsional effect on the response of structures is proposed. In order to verify the efficiency of the proposed index, two single-story and two multistory structures are considered. Regular as well as irregular systems are examined, while double eccentric systems subjected to bidirectional ground motion are considered. The symmetric structures are designed according to the provision imposed by Eurocode 8, where accidental eccentricity is taken into consideration in each direction. The structures studied are torsionally stiff and mass eccentric. In order to assess the performance of the proposed index, nonlinear dynamic analyses are conducted using natural accelerograms belonging to three hazard levels. For the test examples considered, various response quantities are computed and their correlation to the suggested index is examined. The results obtained indicate that, the proposed index provides a reliable quantitative evaluation of the torsional effect on the structural response.

2. Treatment of torsional effect

The basic principles associated with the parameters that characterize the torsional effect on structural behavior as well as their features are briefly described in this section. In case of single-story structures, the rigidity center (CR) is defined as the point on the diaphragm through which a static horizontal force causes only translation on the diaphragm, irrespective of the force direction. While for the case of multistory buildings, the rigidity centers of the stories cannot be defined in a strict manner and many definitions have been proposed so far (Humar 1984, Smith and Vezina

1985, Poole 1977, Cheung and Tso 1986). Indicatively, Humar (1984) defined the location of story rigidity center as the point where the resultant lateral forces of the story, when applied to that point, does not cause rotation of the specific story. Smith and Vezina (1985) defined the location of story rigidity center of multistory buildings for given distribution of the lateral loads, as the point on the story where if the external lateral load is applied no torque is observed.

Based on the undamped equations of motion written for multistory buildings and assuming linear behavior, the coordinates of the rigidity center are given by the following expressions

$$\boldsymbol{x}_{CR} = \frac{\boldsymbol{K}_X \boldsymbol{K}_{Y\theta} - \boldsymbol{K}_{XY} \boldsymbol{K}_{X\theta}}{\boldsymbol{K}_X \boldsymbol{K}_Y - \boldsymbol{K}_{XY}^2} \tag{1a}$$

$$\boldsymbol{y}_{CR} = \frac{\boldsymbol{K}_Y \boldsymbol{K}_{X\theta} - \boldsymbol{K}_{XY} \boldsymbol{K}_{Y\theta}}{\boldsymbol{K}_X \boldsymbol{K}_Y - \boldsymbol{K}_{XY}^2} \tag{1b}$$

where $\boldsymbol{K}_X$, $\boldsymbol{K}_Y$, $\boldsymbol{K}_{XY}$, $\boldsymbol{K}_{X\theta}$ and $\boldsymbol{K}_{Y\theta}$ are submatrices of the building global stiffness matrix corresponding to translational (x and y) and rotational (θ) degrees of freedom of the system (Fig. 1). Eq. (1) do not lead to a unique definition of the story rigidity centers, due to the fact that the product of the operations of the second part of Eq. (1) do not yield in general diagonal matrices. This deficiency is overcome if static lateral loads are introduced as follows

$$\mathbf{x}_{CR} = \left\{\tilde{\mathbf{P}}_Y\right\}^{-1} \frac{\boldsymbol{K}_{Y\theta} - \boldsymbol{K}_{YX} \boldsymbol{K}_X^{-1} \boldsymbol{K}_{X\theta}}{\boldsymbol{K}_Y - \boldsymbol{K}_{YX} \boldsymbol{K}_X^{-1} \boldsymbol{K}_{XY}} \tilde{\mathbf{P}}_Y \tag{2a}$$

$$\mathbf{y}_{CR} = -\left\{\tilde{\mathbf{P}}_X\right\}^{-1} \frac{\boldsymbol{K}_{X\theta} - \boldsymbol{K}_{XY} \boldsymbol{K}_Y^{-1} \boldsymbol{K}_{Y\theta}}{\boldsymbol{K}_X - \boldsymbol{K}_{XY} \boldsymbol{K}_Y^{-1} \boldsymbol{K}_{YX}} \tilde{\mathbf{P}}_X \tag{2b}$$

where $\tilde{\mathbf{P}}_X$ and $\tilde{\mathbf{P}}_Y$ are the vectors of the static lateral loads. Thus, the definition of the coordinates of Eq. (2) are load-dependent (Chopra 1987). However, there is a special class of multistory buildings, called proportional framing buildings, for which the rigidity center, shear center and center of twist coincide, they are load-independent and lie on a vertical line which can be defined (Chopra 1987, Riddel and Vasquez 1984). For the case of single-story systems, the terms of Eq. (1) represent scalar quantities and unique centers of rigidity can be always computed.

The shear center (SC) of single-story system is defined as the point on the diaphragm where the resultant of the shear forces developed at the vertical resisting elements is applied to, while the resultant of the lateral static loads passes through the center of rigidity, causing no rotation of the diaphragm. While the shear center of a floor of a multistory building is defined as the point of the floor where the resultant of the story shear forces at that level passes when the static horizontal loads pass through the centers of rigidity of the floors, causing no twist in any of them. The center of twist of single-story system is defined as the point on the diaphragm that is not subjected to translation but only to twist about it, when a torsional moment is statically applied on the diaphragm. In case of multistory buildings, the center of twist of the floors is defined as the point on the floor diaphragm, which remains stationary when static horizontal torsional moments are applied at the floor levels. Furthermore, the strength center (CV) is defined as the point through which the resultant of the lateral forces passes, while if the story becomes a mechanism no rotation of the diaphragm is introduced. It should be noted that centers of twist, rigidity and shear for single-story structures coincide (Chopra 1987); thus, the coordinates of the shear center and the

center of twist are also obtained from Eq. (1). Mass center (CM) is defined as the point on the diaphragm where the resultant of the inertia forces is applied to. The eccentricity of the above mentioned centers with reference to CM can have a great impact on the structural response.

The most important parameters characterizing the torsional effect on a building for elastic structural behavior are the static eccentricity (e_{CR}) and the ratio of the uncoupled torsional to lateral frequency ratio (Ω). The static eccentricity e_{CR} of single-story structures is defined as the distance between CM and CR. While the static eccentricity e_{CR}^{j} of the j^{th} floor of a multistory building is computed as the distance between its center of mass and its center of rigidity. According to the ratio of the uncoupled torsional to lateral frequency ratio (Ω), buildings are classified as either torsionally-stiff or torsionally-flexible. When the value of Ω exceeds unity, the building is characterized as torsionally-stiff otherwise the building is considered as torsionally-flexible. For torsionally-stiff structures the predominant mode is translational while for torsionally-flexible systems the predominant mode is torsional. Furthermore, the edges of the structures are also denoted as stiff or flexible with reference to the position of the mass and rigidity centers. In particular, when the edge distance from CM is smaller than that from CR, the edge is characterized as flexible otherwise the edge is characterized as stiff. It is worth noting that a building can be torsionally stiff in one direction and flexible in the other. Torsionally stiff buildings display increased displacements at the flexible edge and decreased at the stiff one, compared to the symmetric design, while torsionally flexible buildings do not follow any specific pattern (Marušić and Fajfar 2005, Kyrkos and Anagnostopoulos 2013).

Once a structural element reaches yield, its stiffness changes affecting the period as well as the static eccentricity of the structure. The location of the rigidity center changes as well as the eccentricity of the structure. Based on this observation Paulay (1997) stated that strength eccentricity is a reliable measure for the elastoplastic range. The strength eccentricity is the distance between the mass center CM and the strength center CV.

3. Ratio of Torsion (ROT)

Torsional moments that are developed due to the eccentricity are sustained by the structural system as a pair of shear forces. Thus, the torsional effect on buildings results in torsion-induced displacements via torsion-induced shear forces on the vertical structural elements. When a lateral loading P_i is applied on the diaphragm, shear forces are developed at each vertical resisting element. Fig. 1 shows a simple plan view along with the vertical resisting elements (shear walls) and the corresponding shear forces developed. Without loss of generality the seismic action is considered along one direction only (y direction) in order to better illustrate the concept of the proposed index. Similar expressions can be obtained when applying seismic excitation along x direction only. Furthermore, more details on this explanatory example can be found in the dissertation of Stathi (2014).

The shear forces developed on the vertical resisting structural elements satisfy the following expression

$$\sum_{k=1}^{n}\left|V_{kij}\right| \neq \sum_{k=1}^{n} V_{kij} \tag{4}$$

where n is the number of vertical structural elements, while i and j correspond to the direction of

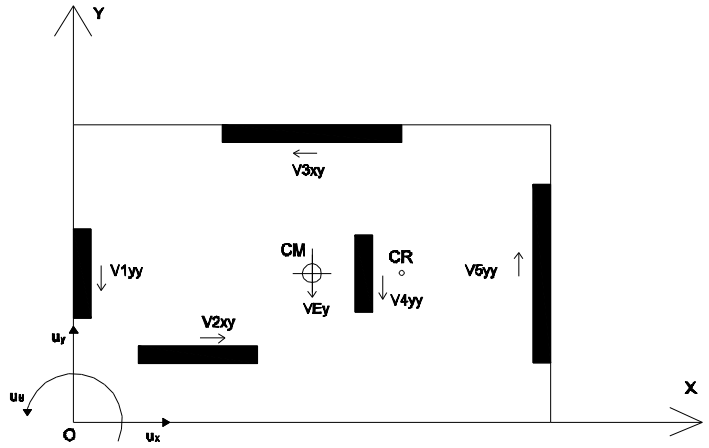

Fig. 1 A typical plan view with shear walls denoting the degrees of freedom of the system

the shear forces of the element *k* and the seismic excitation with reference to the structural axes, respectively. Eq. (4) denotes that the sum of the absolute values of the shear forces differs from their algebraic sum. This observation is attributed to the torsional contribution of the shear forces, since the torsional moment is sustained by the system as a pair of opposing shear forces. For the plan view of Fig. 1 and seismic action along *y* direction only, the following relations are satisfied

$$\sum_{k=1}^{n}\left|V_{kxy}\right| \neq \sum_{k=1}^{n} V_{kxy} = 0 \tag{5}$$

$$\sum_{k=1}^{n}\left|V_{kyy}\right| \neq \sum_{k=1}^{n} V_{kyy} = V_{Ey} \tag{6}$$

where V_{Ey} is the base shear along *y* direction.

The torsion induced to the floor is usually computed from the shear forces of the structural elements, while the elements' torsional moments are neglected. Based on the observations described above an index is proposed in this study, called ratio of torsion (*ROT*) that represents a measure to quantify the torsional effect.

For demonstration purposes and without loss of generality the simplified model of Fig. 2 is adopted. It is assumed that the lateral force resistance of the structure is provided by shear walls only, while floor diaphragm is considered rigid. The system is mono-symmetric with reference to *x* direction and the eccentricity is introduced to the system by asymmetric mass distribution. The response of the system is considered for earthquake loading.

In Fig. 2, shear forces induced by translation are denoted as V'_{kiy}, while the torsional component as V''_{kiy}. The locations of CM and CR together with the stiffness eccentricity e_{CRX} along *x* direction are also shown in Fig. 2. The twist of the diaphragm is the result of the torque M_t induced by the story base shear V_{Ey}. This torque affects the shear forces developed on vertical resisting elements. Consequently, the shear forces developed consist of two components, the translational and rotational one. The translational shear force component of element *k* denoted as V'_{kiy} is calculated by

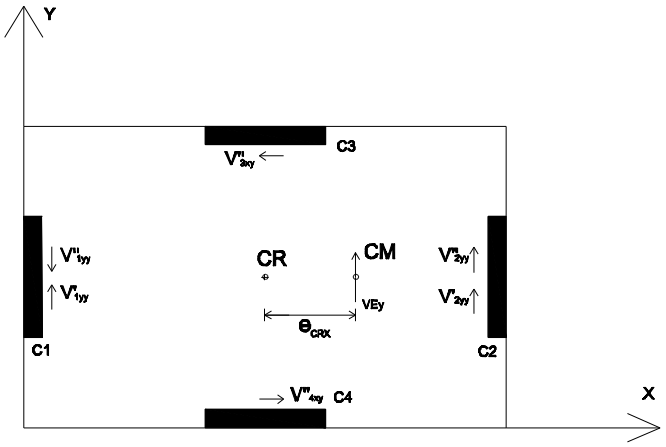

Fig. 2 Plan view of location of CM and CR

$$V_{kiy}^{'} = \frac{k_{ky}}{\sum_{k=1}^{n} k_{ky}} V_{Ey} \tag{7}$$

where V_{Ey} is the design base shear along the y direction, k_{ky} is the translational stiffness of the element k along y direction, n denotes the number of the vertical resisting elements and i the direction of the shear force of the element k. The torsional component of shear force is given by

$$V_{kiy}^{"} = x_k k_{ky} \frac{M_t}{K_t} \tag{8}$$

where x_k is the distance between the vertical resisting element k and CR, M_t is the torque introduced by the design shear force V_{Ey}, while K_t represents the torsional stiffness of the system calculated according to the relationship

$$K_t = \sum y_k^2 k_{kx} + \sum x_k^2 k_{ky} \tag{9}$$

The total shear force for element k is obtained by

$$V_{kiy} = V_{kiy}^{'} + V_{kiy}^{"} \tag{10}$$

Similar expressions to Eqs. (9) to (11) can be written for x direction as well.

The general expression of ROT for a specific time step t is defined as

$$ROT(t) = \frac{\sum_{k=1}^{n} \sum_{i=x,\, j=y}^{y,x} \left|V_{kij}(t)\right| - \left|V_{Ex}(t)\right| - \left|V_{Ey}(t)\right|}{\left|V_{Ex}(t)\right| + \left|V_{Ey}(t)\right|} \tag{11}$$

where for simplification reasons the time step t is excluded in the description that follows. The proposed expression for *ROT* is based on the sum of absolute values of torsion-induced shear forces developed on the structural elements normalized to the base shear which is imposed to the structure by the seismic action. In this way, the amplification of the imposed base shear V_{Ey} due to torsion is quantified. It should be noted that for the special case that Eq. (6) becomes equality ROT formulation is not affected, since the difference between the sum of the absolute value of shear forces and their algebraic sum is equal to zero and consequently its contribution to the numerator of ROT formulation is also zero.

In the case of the unidirectional seismic ground motion along y axis considered, the structural elements resisting along the transverse direction x usually contribute to the torsional stiffness in the elastic range. Consequently, only torsion-induced shear forces are developed in these elements (Paulay 1997). In this case using Eq. (11) *ROT* becomes

$$ROT = \frac{\left|V_{1yy}^{'} - V_{1yy}^{"}\right| + \left|V_{2yy}^{'} + V_{2yy}^{"}\right| + \left|V_{3xy}^{"}\right| + \left|V_{4xy}^{"}\right| - \left|V_{Ey}\right|}{\left|V_{Ey}\right|} \tag{12}$$

The static equilibrium of forces acting on the diaphragm of the structure is given by

$$\left|V_{Ey}\right| = \left|V_{1yy}^{'} - V_{1yy}^{"}\right| + \left|V_{2yy}^{'} + V_{2yy}^{"}\right| \tag{13}$$

Therefore, substituting Eq. (13) in Eq. (12), the *ROT* becomes

$$ROT = \frac{\left|V_{1yy}^{'} - V_{1yy}^{"}\right| + \left|V_{2yy}^{'} + V_{2yy}^{"}\right| + \left|V_{3xy}^{"}\right| + \left|V_{4xy}^{"}\right| - \left|V_{1yy}^{'} - V_{1yy}^{"}\right| - \left|V_{2yy}^{'} + V_{2yy}^{"}\right|}{\left|V_{1yy}^{'} - V_{1yy}^{"}\right| + \left|V_{2yy}^{'} + V_{2yy}^{"}\right|} \tag{14}$$

or

$$ROT = \frac{\left|V_{3xy}^{"}\right| + \left|V_{4xy}^{"}\right|}{\left|V_{1yy}^{'} - V_{1yy}^{"}\right| + \left|V_{2yy}^{'} + V_{2yy}^{"}\right|} \tag{15}$$

which can be written in a compact form as

$$ROT = \frac{\left|V_{3xy}^{"}\right| + \left|V_{4xy}^{"}\right|}{\left|V_{Ey}\right|} \tag{16}$$

The numerator of Eq. (16) represents the sum of the absolute values of the additional torsion-induced shear forces and the denominator represents the base shear imposed by the seismic excitation. ROT belongs to the cumulative indices, since the shear component of each individual element is added and subsequently the base shear is subtracted in order to obtain the total amount of torsional amplification. Thus, the total amount of torsional effect is significantly larger than that of each individual element. This divergence increases as the number of elements of the structure increases.

In order to implement the proposed index to multistory buildings, Eq. (11) is calculated for every story of the building and the global value of the index is defined as the sum of the *ROT* value at each story

Table 1 Natural records (Somerville and Collins 2002)

Earthquake	Station	Distance	Site
Records in 50/50 hazard level			
Honeydew (PT) 17 August 1991	Cape Mendocino	20	rock
	Petrolia	17	soil
Cape Mendocino (CM) 25 April 1992	Rio Dell	13	soil
	Butler Valley	37	rock
Cape Mendocino (C2) aftershock, 4/26/92	Fortuna	43	soil
	Centerville	28	soil
Records in 10/50 hazard level			
Tabas (TB) 16 September 1978	Dayhook	14	rock
	Tabas	1.1	rock
Cape Mendocino (CM) 25 April 1992	Cape Mendocino	6.9	rock
	Petrolia	8.1	soil
Chi-Chi (CC), Taiwan 20 September 1999	TCU101	4.9	soil
	TCU102	3.8	soil
Records in 2/50 hazard level			
Valparaiso (VL), Chile 3 May 1985	Vina del Mar	30	soil
	Zapaller	30	rock
Michoacan (MI), Mexico 19 September 1985	Caleta de Campos	12	rock
	La Union	22	rock
	La Villita	18	rock
	Zihuatenejo	21	rock

$$ROT = \sum_{m=1}^{l} ROT_m \tag{17}$$

where l is the number of the building stories.

The main advantage of the proposed index is that it provides the amount of amplification of shear forces due to the torsional effect in a quantitative manner, since it provides the percentage of amplification of total shear forces developed on vertical structural elements in comparison to its symmetric counterpart and proved to be efficient and reliable for all states of response. Compared to other structural response quantities related to torsion, such as base torque, it is consistent with this quantity without requiring to perform additional analyses in order to draw to conclusions regarding the influence of the torsional effect on the structural response with regard to upper diaphragm rotation it proved to be not consistent with values of base torque and thus not reliable. For example, if for the case of an eccentric building the *ROT* value is equal to 60% means that the sum of the shear forces of its vertical structural resisting members were increased by 60% in comparison to its symmetric counterpart. Furthermore, minimizing the numerator of Eq. (16) that corresponds to the sum of the absolute values of the additional torsion-induced shear forces improved designs can be achieved. Moreover, it is easily calculated since *ROT* is computed using

the shear forces developed on the vertical structural elements.

4. Numerical modeling

In order to perform nonlinear static or dynamic structural analyses the plastic hinge or the fiber approach can be adopted in the regions where inelastic deformations are expected to be developed. The fiber beam-column approach (Fragiadakis and Papadrakakis 2008) is implemented in this study since plastic hinge approach has limitations in terms of accuracy. According to the fiber approach, each structural element is discretized into a number of integration sections restrained to the beam kinematics and each section is divided into a number of fibers with specific material properties. Every fiber in the section can be assigned to different material properties, e.g., concrete, structural steel, or reinforcing bar, while the sections are located at the Gaussian integration points of the elements. The main advantage of the fiber approach is that every fiber has a simple uniaxial material model allowing an easy and efficient implementation of the inelastic behavior. The shortcoming of this approach related to the existence of shear deformations can be alleviated with the incorporation of a triaxial law taking into consideration axial and shear interaction (Papachristidis *et al.* 2010). In the numerical test examples considered in this study, all analyses have been performed using the OpenSEES platform (McKenna and Fenves 2001). A bilinear material model with pure kinematic hardening is adopted for the structural steel. For the simulation of the concrete the modified Kent-Park model is applied, where the monotonic envelope of concrete in compression follows the model of Kent and Park (1971) as extended by Scott *et al.* (1972). This model allows an accurate prediction of the capacity for flexure-dominated RC members despite its relatively simple formulation.

5. Numerical examples

The performance of the test examples considered in this study is assessed with reference to their structural behavior, in connection to interstorey drifts, displacements, columns' shear forces, base torque and upper diaphragm's rotation, for different seismic hazard levels. For this purpose a number of nonlinear time history analyses have been carried out by applying six natural records for each hazard level (50/50, 10/50 and 2/50) chosen from Somerville and Collins (2002) (see Table 1). The records of each hazard level are scaled to the same PGA in order to ensure compatibility between the records, in accordance to the hazard curve taken from the work by Papazachos *et al*. (1993) (see Table 2). Eighteen nonlinear dynamic analyses have been performed for each design in order to assess the performance of the structure for all records and hazard levels.

Table 2 Seismic hazard levels (Papazachos *et al*. 1993)

Event	Recurrence Interval	Probability of Exceedance	PGA (g)
Frequent	21 years	90% in 50 years	0.06
Occasional	72 years	50% in 50 years	0.11
Rare	475 years	10% in 50 years	0.31
Very Rare	2475 years	2% in 50 years	0.78

In order to assess the efficiency of the proposed index the maximum *ROT* value is compared to the maximum values of quantities related to torsion and to other structural response quantities in a number of characteristic numerical examples for different levels of seismic intensity. In particular, two single-story and two four-story torsionally stiff test examples are considered. They are horizontally regular and irregular, exhibiting double eccentricity. Furthermore, three different distributions of the mass were considered for every test example, corresponding to 5%, 10% and 20% eccentricity. In all test examples the following material properties are assumed: Concrete C20/25 with modulus of elasticity equal to 30 GPa and characteristic compressive cylinder strength equal to 20 MPa, longitudinal and transverse steel reinforcement B500C with modulus of elasticity equal to 210 GPa and characteristic yield strength equal to 500 MPa. The design spectrum used correspond to soil type B (characteristic periods T_B=0.15 sec, T_C=0.50 sec and T_D=2.00 sec). Moreover, the importance factor γ_I was taken equal to 1.0, while the damping correction factor η is equal to 1.0, since a damping ratio of 5% has been considered. The symmetric design is denoted as *sym*, while the mass eccentric designs are denoted as *ecc0.05*, *ecc0.10* and *ecc0.20* corresponding to 5%, 10% and 20% eccentricity, respectively.

The eccentricity is introduced by assuming non-uniform mass distribution, which results into different location of the mass center, while the center of rigidity coincides with their geometric center. The response quantities and proposed index values obtained for the eccentric designs were compared to those obtained for the corresponding symmetric one. All test examples are classified as torsionally stiff, since the value of the uncoupled frequency ratio is greater than unity. The first three periods of vibration and the uncoupled frequency ratios are listed for all test examples in Tables 3-6. In order to study the reliability of the proposed index for all states of response (elastic or elastoplastic) the natural accelerograms of Table 1 are applied and the results presented in this study correspond to maximum values obtained from the time-history analyses performed for each hazard level.

Table 3 Test example 1 - Vibration periods and uncoupled frequency ratios

	T_1	T_2	T_3	$\Omega_x = \frac{\omega_t}{\omega_x}$	$\Omega_y = \frac{\omega_t}{\omega_y}$
sym	0.3593^x	0.3484^y	0.2526^t	1.4224	1.3793
ecc0.05	0.3620^x	0.3512^y	0.2524^t	1.4342	1.3914
ecc0.10	0.3753^x	0.3539^y	0.2519^t	1.4898	1.4049
ecc0.20	0.4320^x	0.3549^y	0.2509^t	1.7218	1.4145

Table 4 Test example 2 - Vibration periods and uncoupled frequency ratios

	T_1	T_2	T_3	$\Omega_x = \frac{\omega_t}{\omega_x}$	$\Omega_y = \frac{\omega_t}{\omega_y}$
ecc	0.3212^x	0.3207^y	0.2243^t	1.4320	1.4297
ecc0.05	0.3263^x	0.3207^y	0.2119^t	1.5398	1.5134
ecc0.10	0.3396^x	0.3207^y	0.2124^t	1.5988	1.5098
ecc0.20	0.3871^x	0.3207^y	0.2155^t	1.7962	1.4881

Table 5 Test example 3 - Vibration periods and uncoupled frequency ratios

	T_1	T_2	T_3	$\Omega_x = \frac{\omega_t}{\omega_x}$	$\Omega_y = \frac{\omega_t}{\omega_y}$
sym	0.9431^x	0.8486^y	0.5998^t	1.5724	1.4148
ecc0.05	0.9464^x	0.8063^y	0.5711^t	1.6572	1.4118
ecc0.10	0.3753^x	0.3539^y	0.2519^t	1.4898	1.4049
ecc0.20	1.0648^x	0.8996^y	0.6097^t	1.7464	1.4755

Table 6 Test example 4 - Vibration periods and uncoupled frequency ratios

	T_1	T_2	T_3	$\Omega_x = \frac{\omega_t}{\omega_x}$	$\Omega_y = \frac{\omega_t}{\omega_y}$
ecc	1.0074^x	1.0059^y	0.6988^t	1.4416	1.4395
ecc0.05	1.0218^x	1.0074^y	0.7006^t	1.4585	1.4379
ecc0.10	1.0633^x	1.0074^y	0.6851^t	1.5520	1.4704
ecc0.20	1.1933^x	1.0074^y	0.6313^t	1.8902	1.5958

5.1 Test example 1

The first test example is a 3D single-story structure subjected to bidirectional seismic excitation, shown in Fig. 3 along with its CM and some features for the eccentric designs. The normalized maximum values with respect to the symmetric design of the shear forces developed at the vertical resisting elements along the *y* direction are provided in Fig. 4 and the corresponding normalized diaphragm displacements are shown in Fig. 5. The trend observed for the interstorey drifts coincide with that of the displacements and therefore they are omitted due to space limitation. The observed trend for torsionally stiff buildings is confirmed in this case for the elastic state of response. Reduced values are developed for the displacements and shear forces along *y* direction for the structural elements located at the stiff side (i.e., col1 and col6) and increased values for the elements located at flexible edge (i.e., col11 and col16) as shown in Figs. 4 and 5. Similar behavior is observed along *x* direction. Once the system enters the elastoplastic state and elements start yielding, as in the case of 2/50 hazard level, the location of the rigidity center cannot been defined since the stiffness does not remain constant and therefore it is not possible to define accurately the flexible and stiff side of the system.

Figs. 6(a)-(c) depict the trend of the base torque, diaphragm rotation and *ROT* values calculated for the three hazard levels considered. The base torque, diaphragm rotation and *ROT* values increase proportionally to the magnitude of eccentricity for all states of response. The calculation of *ROT* is based on internal shear forces for each hazard level and can be directly correlated to the amplification of the shear forces developed on the vertical structural elements due to torsional effect. Taking into account that torque is sustained by a system as pairs of shear forces whose resultant is zero, higher *ROT* values indicate higher effect of torsional effect on the structural elements. For the symmetric system, *ROT* magnitude is zero or almost zero for all states of response, while for the system characterized by 20% eccentricity (*ecc0.20*) the shear forces were amplified by more than four times due to torsion for the 10/50 hazard level (Fig. 6(b)) and six

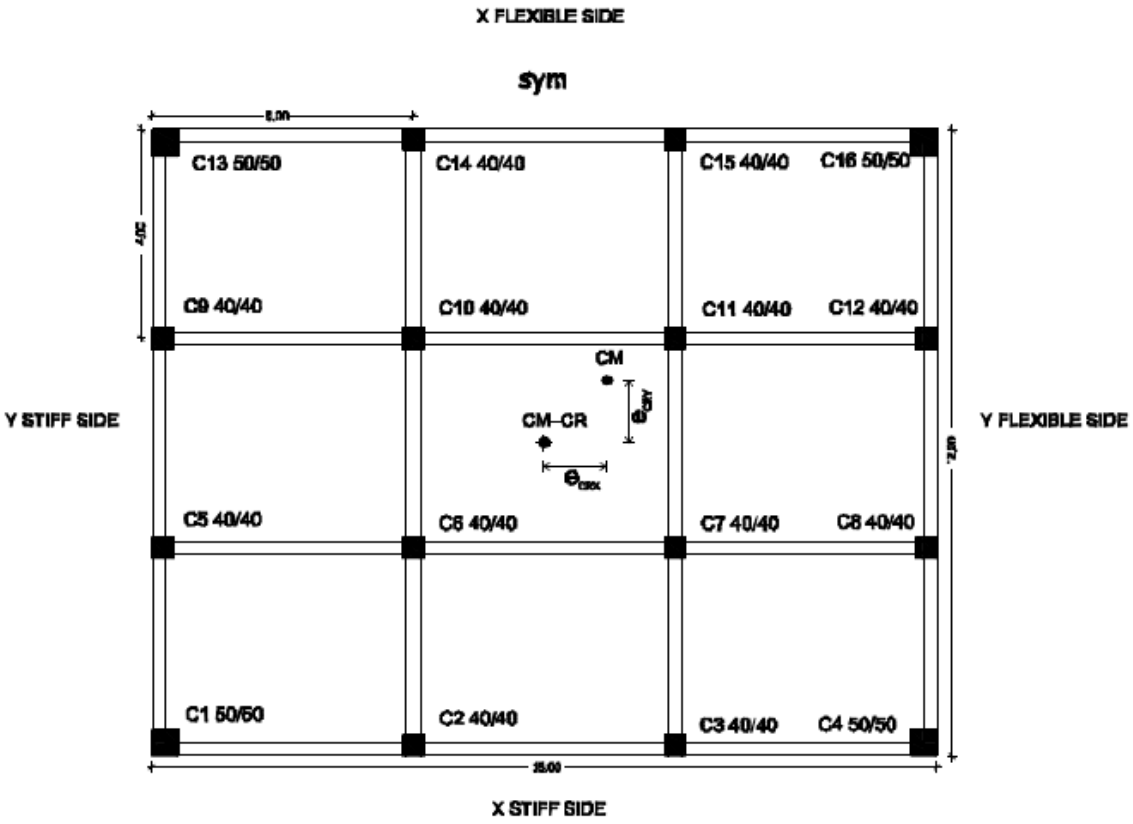

Fig. 3 Test example 1 - plan view

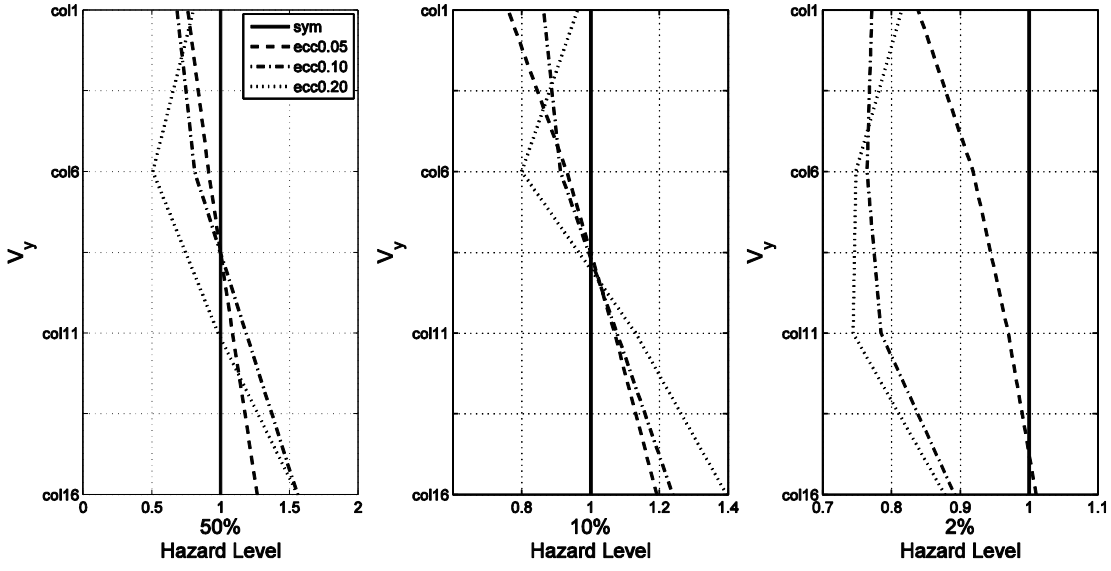

Fig. 4 Test example 1-Normalized shear forces along *y* direction for each design and hazard level

times for the case of 2/50 (Fig. 6(c)). These figures revealed that the trend of maximum base torque and that of maximum diaphragm rotation is not always in accordance to each other. Figs. 6(a) and 6(b) show that for the case of *ecc0.20* design, a decrease of the maximum diaphragm rotation is observed for 10/50 to 2/50 hazard levels, whereas the maximum base torque values are increased for the corresponding states. Furthermore, ROT index follows the trend of the base torque values. It is worth mentioning that ROT value is not equal to zero in the symmetric case for 10/50 and 2/50 hazard levels. This is attributed to the yielding of the elements when the structural elements enters elastoplastic and plastic states of response. The stiffness of the elements is affected leading to changes on the system eccentricity compared to its initial one. The effect of the eccentricity can also be observed to the other response quantities related to torsion, such as base torque and diaphragm rotation, but their increase is too small to be seen on the graph. All response values related to torsion are provided in Table 7. Finally, it should be clarified that when the structures enters elastoplastic and plastic states of response, there are elements still behaving in the elastic range. Moreover, the shear force of the elements that have yielded is not constant due to unloading and reloading. This affects ROT value, which is not constant during nonlinear state of response as expected.

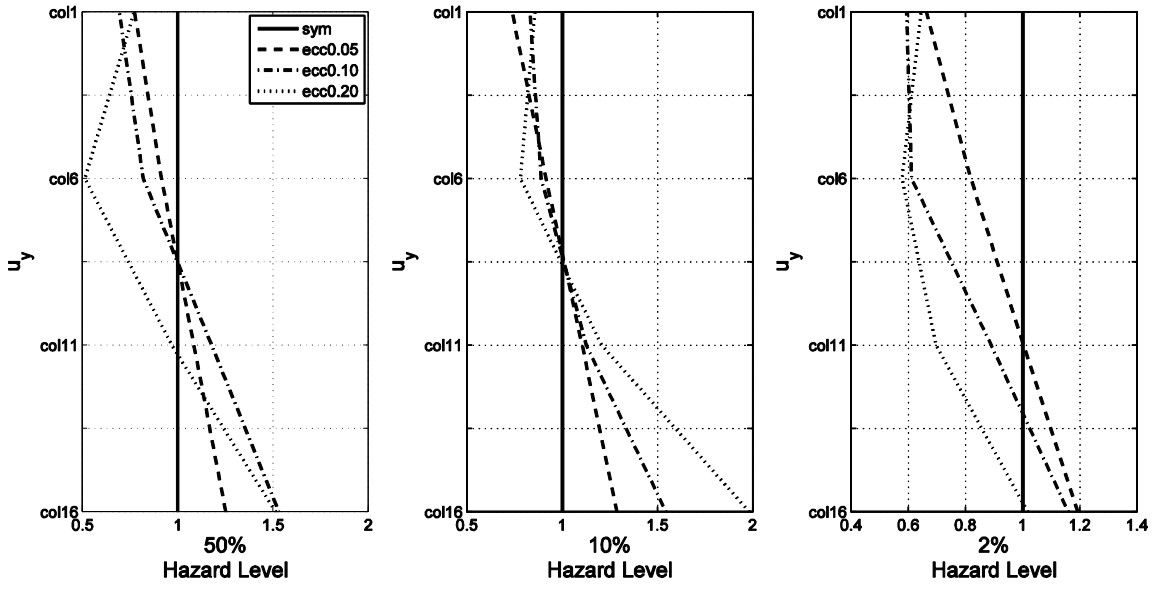

(a) (b) (c)

Fig. 5 Test example 1-Normalized displacement values along *y* direction for each design and hazard level

Table 7 Symmetric design - Base torque, diaphragm rotation and ROT values for all hazard levels

Symmetric design	Hazard Levels		
	50/50	10/50	2/50
ROT	8.78E-03	1.66E-01	3.99E-01
Base Torque	5.66E-08	1.16E-02	5.60E-02
Diaphragm Rotation	5.76E-12	1.62E-07	8.40E-07

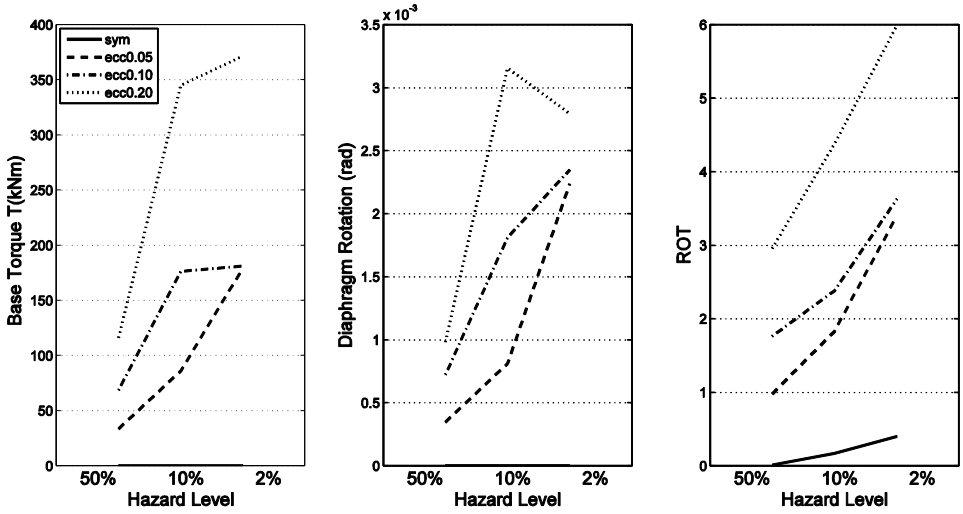

Fig. 6 Test example 1, (a) Base torque, (b) diaphragm rotation and (c) ROT

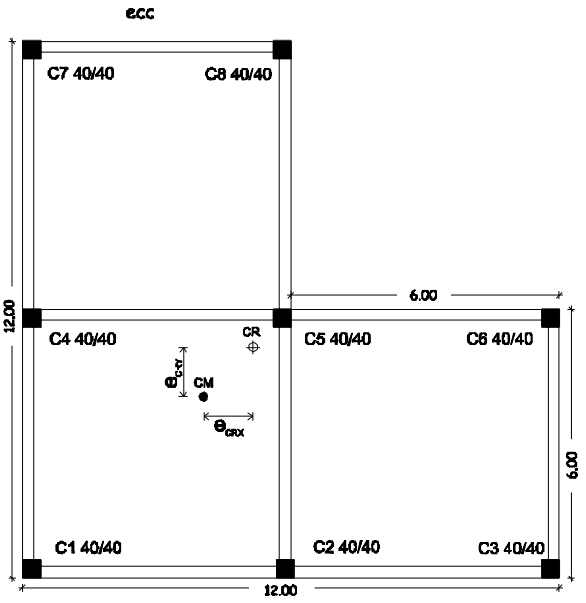

Fig. 7 Test example 2 - plan view

5.2 Test example 2

The second example, shown in Fig. 7, is a horizontally irregular single-story structure with bidirectional eccentricity subjected to two-component ground motion. For this test example it was not possible to define a symmetric design according to the regulations imposed by the design codes. Consequently, a small amount of eccentricity 0.83% is noticed for the reference design that

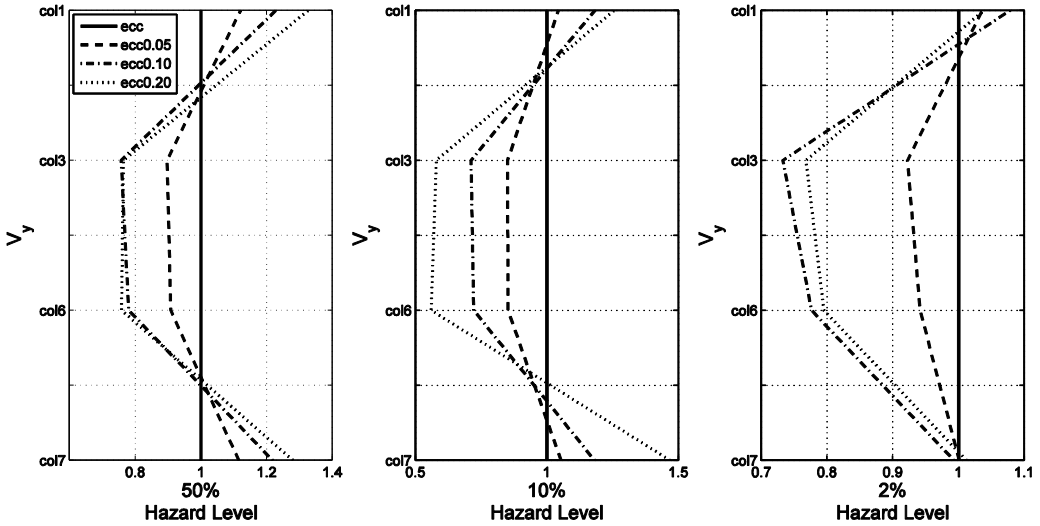

(a) (b) (c)

Fig. 8 Test example 2-Normalized shear forces along *y* direction for each design and hazard level

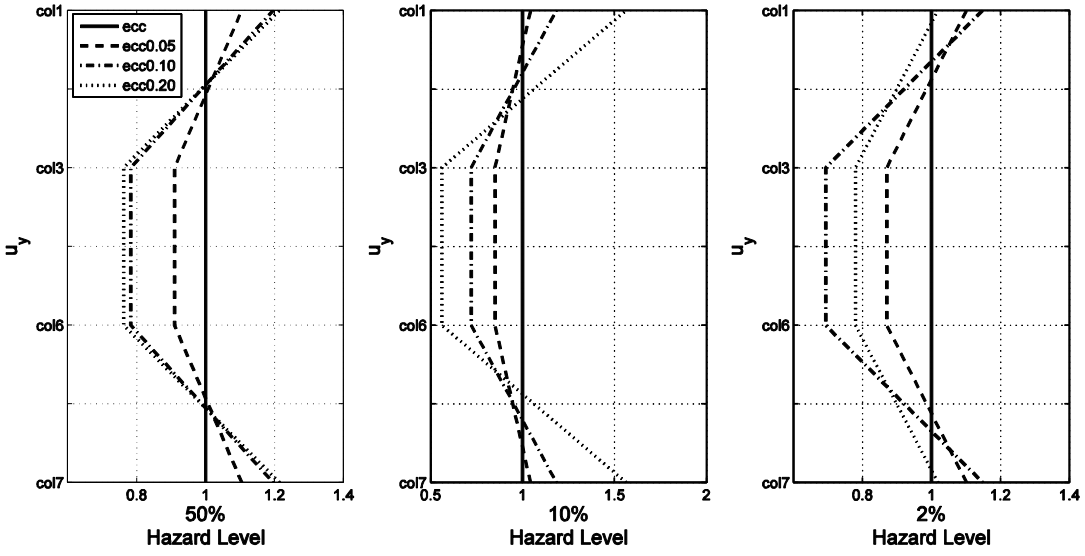

(a) (b) (c)

Fig. 9 Test example 2-Normalized displacement values along *y* direction for each design and hazard level

is denoted as "*ecc*", instead of the notation "*sym*" used for the previous test example. The other alternative designs considered have the same eccentricities as the previous example (i.e., 5%, 10% and 2%), while the characteristic response quantities (shear forces and displacements - interstorey drifts have the same trend with displacements and therefore they are excluded due to space limitation) corresponding to direction *y* are used for comparison. Figs. 8 and 9 show the increase of the response quantities, for the elements located at the flexible edge (i.e., col1 and col7) and the

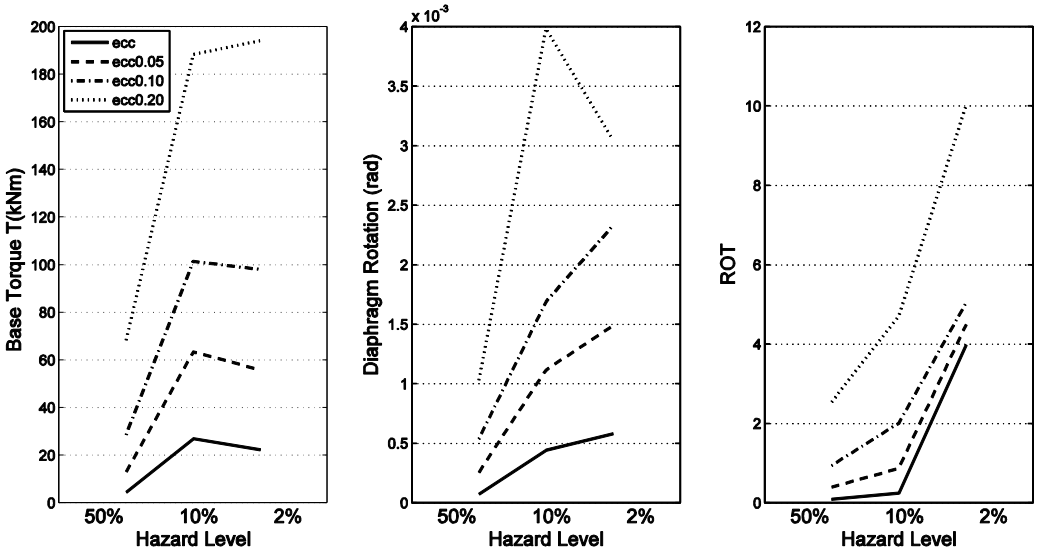

Fig. 10 Test example 2, (a) Base torque, (b) diaphragm rotation and (c) ROT

decrease for those located at the stiff edge (i.e., col3 and col6).

As can be seen in Fig. 10, almost zero values were obtained for base torque, diaphragm rotation and *ROT* for the elastic state of response (i.e., 50/50 hazard level) for the "*ecc*" design. For the eccentric designs, the corresponding values are increased proportionally to the eccentricity. Similar observations are obtained for the other two hazard levels. Although a slight increase is observed on the magnitude of base torque, a significant increase for *ROT* values was noticed for the 10/50 and 2/50 hazard levels. It is worth noting that for the 5% eccentricity design, increased *ROT* value is noticed for 2/50 hazard level as shown in Fig. 10(c). Moreover, despite the fact that a very small decrease of base torque was observed for *ecc*, *ecc0.05* and *ecc0.10* designs, a significant increase was noticed for the corresponding ROT values. This is attributed to the asymmetric yielding of the vertical resisting elements due to the asymmetric plan view of the structure. The trend with respect to the behavioral quantities observed for the torsionally stiff horizontally regular systems has been confirmed also for torsionally stiff horizontally irregular systems.

5.3 Test example 3

A four-story building is implemented in the current test example, which possesses the same layout as test example 1. A two-component seismic excitation is imposed to all cases, while the following response quantities refer to the structural elements of the upper story. As it is shown in Fig. 11, the shear forces at the stiff edge along the *y* direction (i.e., col1 and col6) are decreased proportionally to the eccentricity, while they are increased at the flexible edge (i.e., col11 and col16). Similar observations can be drawn for the displacements and interstorey drifts (see Figs. 12-13). As can be noticed in Table 5, the uncoupled torsional to translational frequency ratio for all designs exceeds unity which implies that they are torsionally stiff. With increased eccentricity, the response quantities for columns at stiff edge (col1, col6) are decreased and for columns at

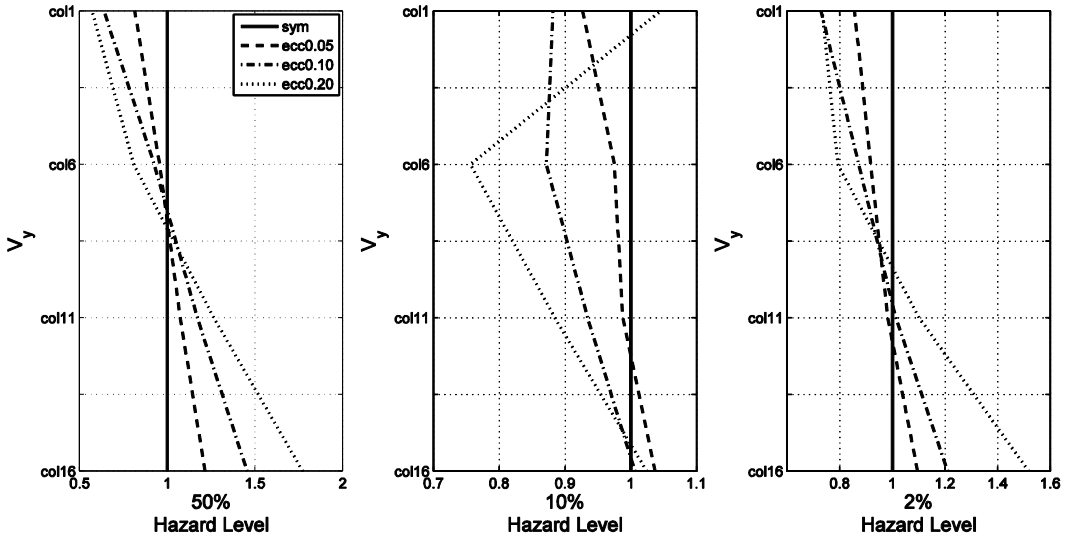

Fig. 11 Test example 3-Normalized shear forces along *y* direction for each design and hazard level

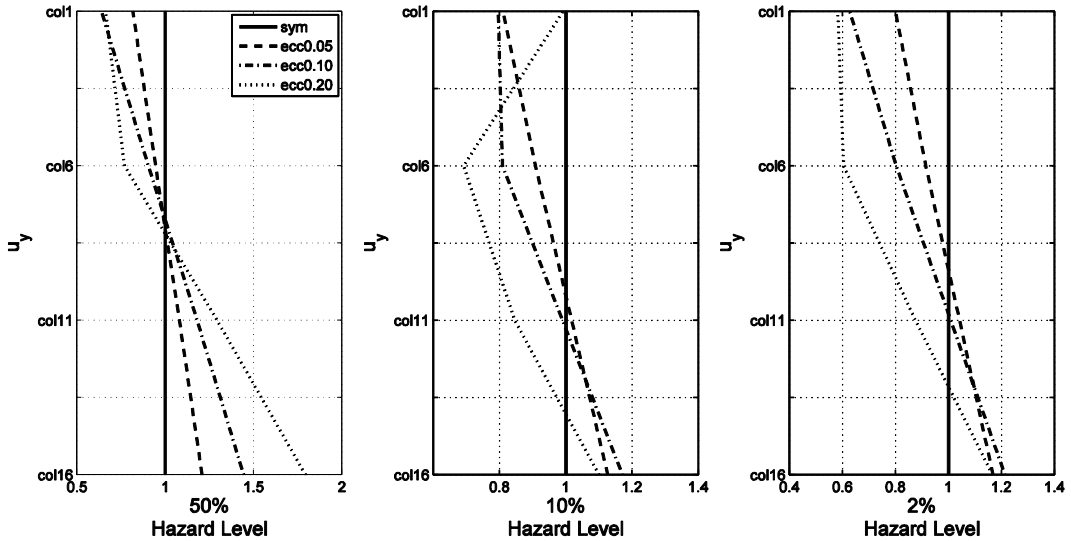

Fig. 12 Test example 3 -Normalized displacement values along *y* direction for each design and hazard level

flexible edge (col11, col16, see Figs. 11-13,) are increased confirming the observed behavior of torsionally stiff systems.

As far as the torsional response quantities are concerned, upper diaphragm's rotation, base torque and *ROT* are increased for all states of response when eccentricity is increased. Their absolute values are shown in Figs. 14. As it can be noticed also in this case, *ROT* values distribution is in accordance with base torque values distribution.

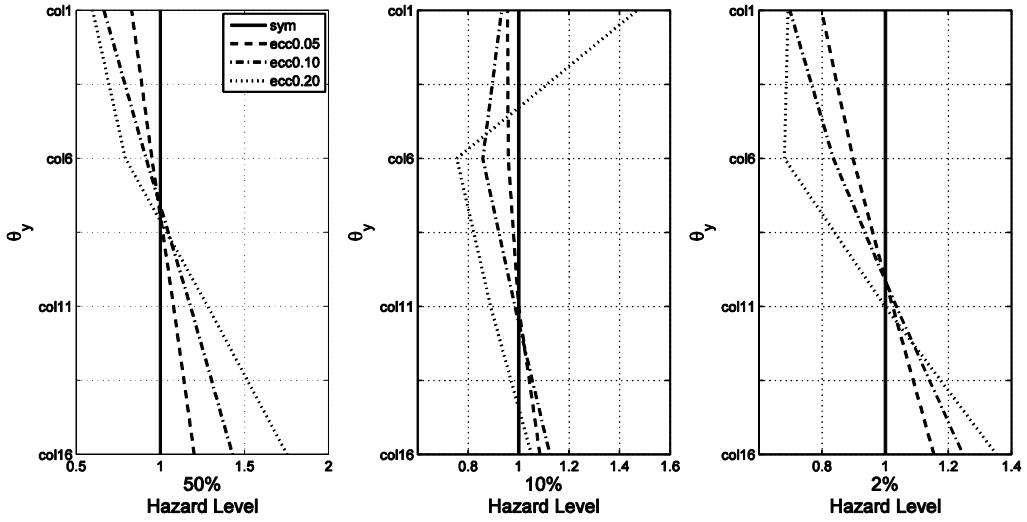

(a) (b) (c)

Fig. 13 Test example 3-Normalized interstorey drift values along *y* direction for each design and hazard level

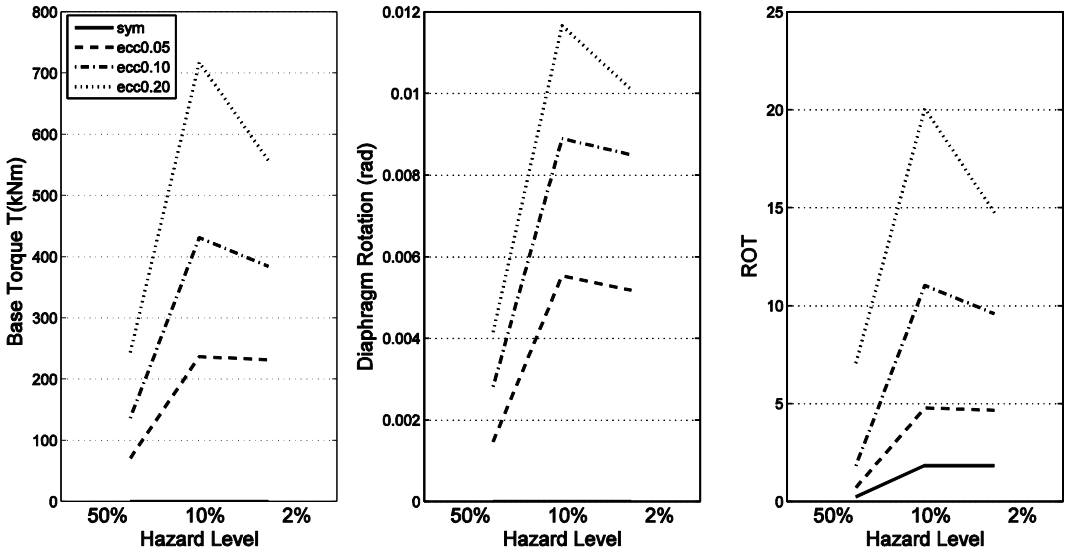

(a) (b) (c)

Fig. 14 Test example 3, (a) Base torque, (b) diaphragm rotation and (c) ROT

5.4 Test example 4

The fourth test example examined in this study is the horizontally irregular four-story building with bidirectional eccentricity subjected to two-component seismic excitation, while its layout is equal to that of test example 2. As in previous example due to its irregular layout, it was not possible to define the symmetric design that complies with the restrictions imposed by the design

codes. The reference design exhibit static eccentricity of 0.8% and is denoted as *ecc*, while the non-symmetric designs considered exhibit the same eccentricity as in the previous examples (i.e., 5%, 10% and 20%). The response quantities studied (shear forces, displacements and interstorey drifts) are presented along *y* direction and refer to the structural elements of the upper story. Similar results are obtained in *x* direction. As it can be seen in Figs. 15-17, the response quantities for elements at the flexible edge (i.e., col1 and col7) are increased while for those at stiff edge (col3, col6) are decreased proportionally to the increase of the eccentricity.

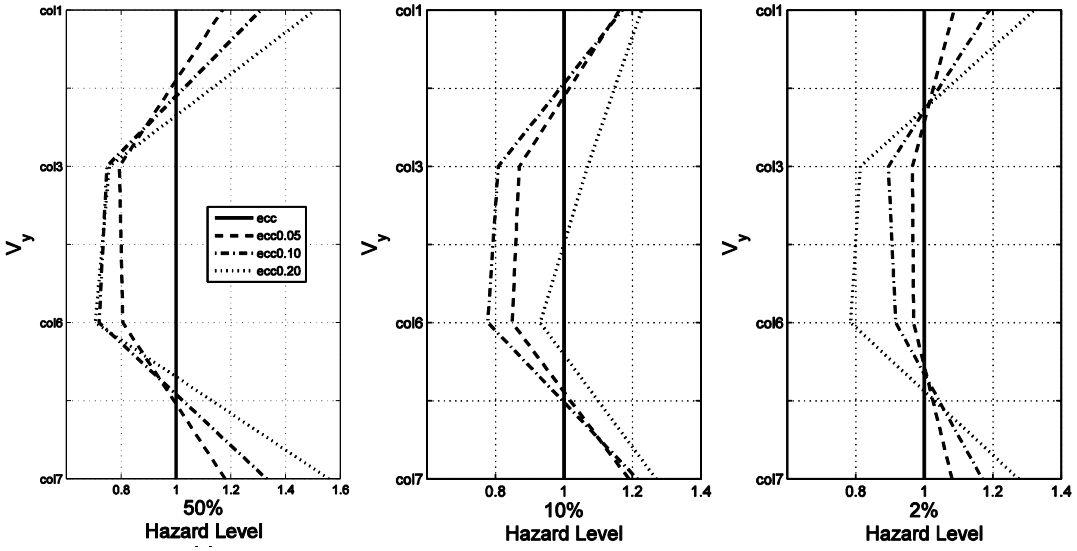

(a) (b) (c)

Fig. 15 Test example 4-Normalized shear forces along *y* direction for each design and hazard level

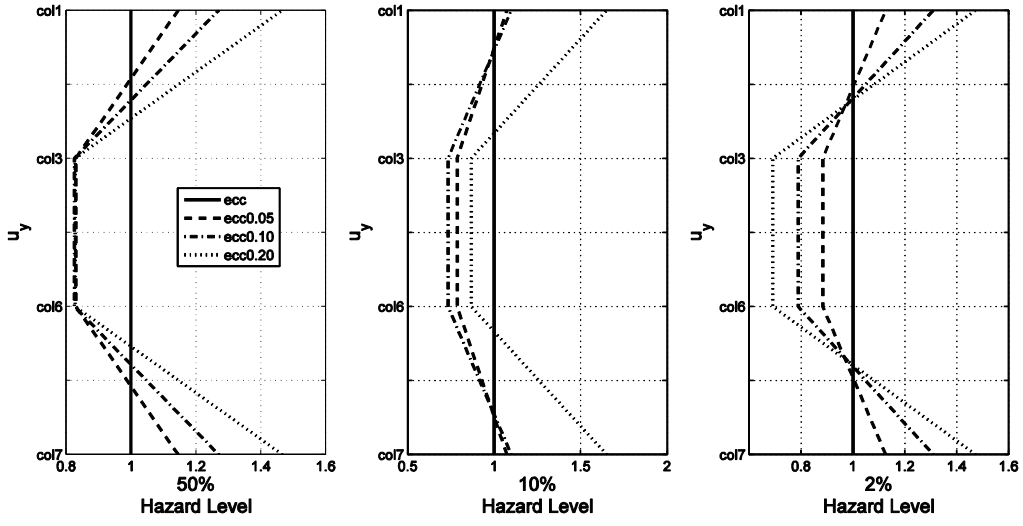

(a) (b) (c)

Fig. 16 Test example 4-Normalized displacement values along *y* direction for each design and hazard level

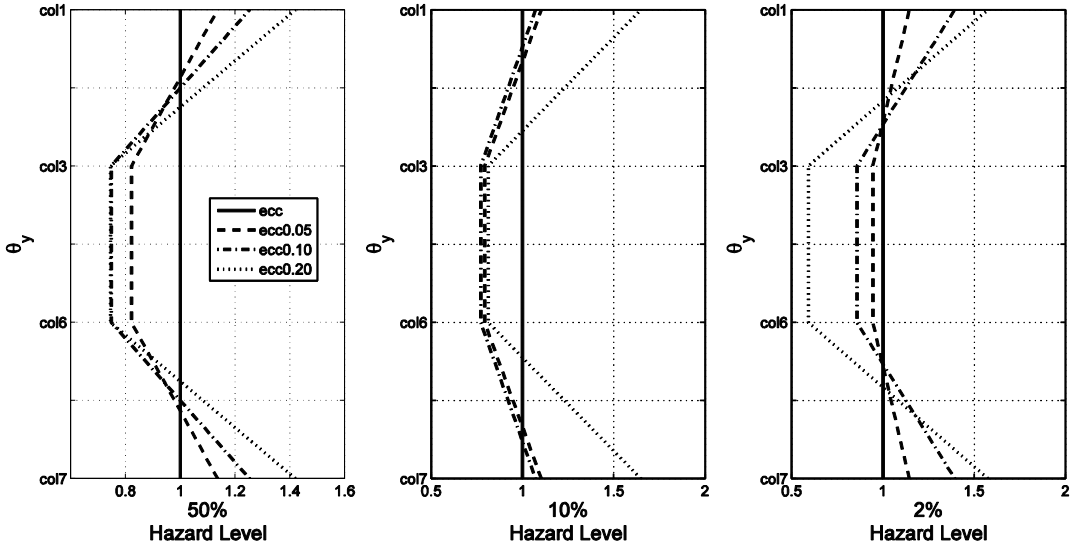

(a) (b) (c)

Fig. 17 Test example 4 -Normalized interstorey drift values along *y* direction for each design and hazard level

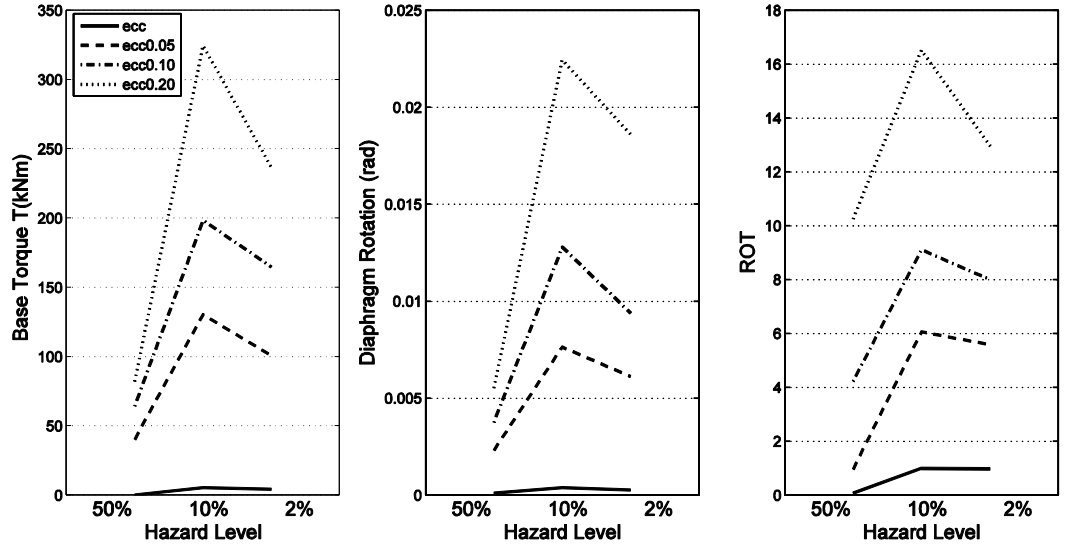

(a) (b) (c)

Fig. 18 Test example 4-(a) Base torque, (b) diaphragm rotation and (c) *ROT*

Similar observations to the previous test examples are also obtained. In particular, for *ecc* design, almost zero base torque, upper diaphragm's rotation and *ROT* values are obtained for the elastic state of response (i.e., for the 50/50 hazard level), while for the non-symmetric designs the corresponding values are increased proportionally to the increase of the eccentricity for all hazard levels (see Fig. 18).

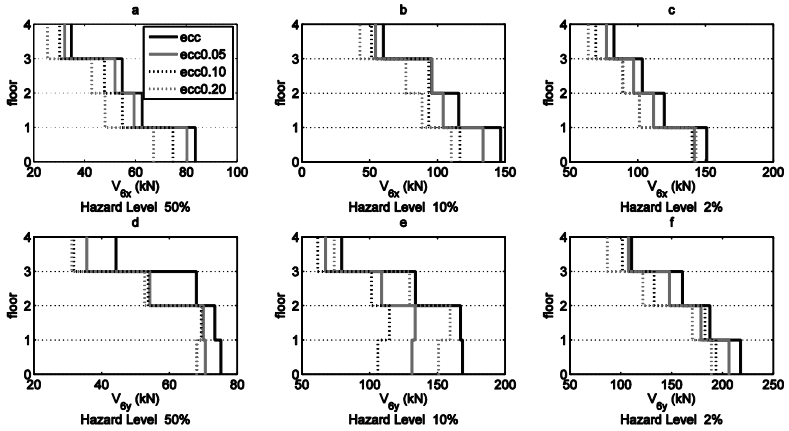

Fig. 19 Test example 4-Column 6 maximum absolute shear force values along *x* (a, b, c) and *y* (d, e, f) direction for all floors and hazard levels

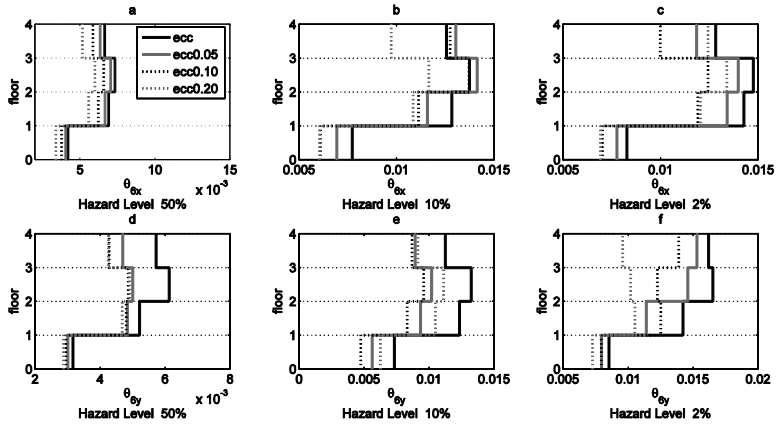

Fig. 20 Test example 4-Column 6 maximum drift values values along *x* (a, b, c) and *y* (d, e, f) direction for all floors and hazard levels

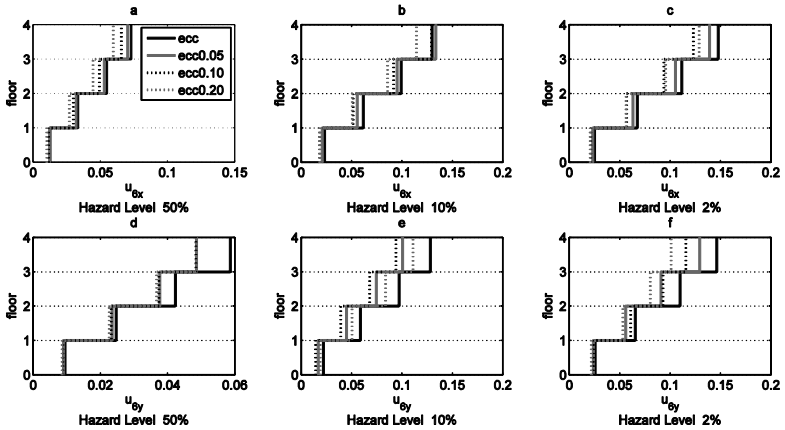

Fig. 21 Test example 4-Column 6 maximum absolute displacements values values along *x* (a, b, c) and *y* (d, e, f) direction for all floors and hazard levels

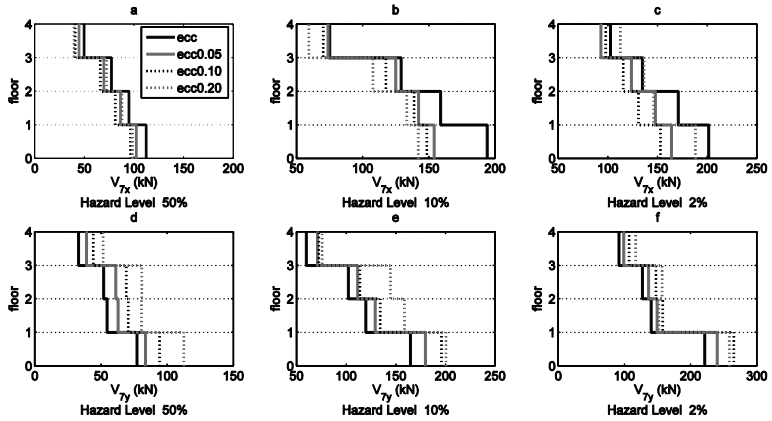

Fig. 22 Test example 4-Column 7 maximum absolute shear force values along *x* (a, b, c) and *y* (d, e, f) direction for all floors and hazard levels

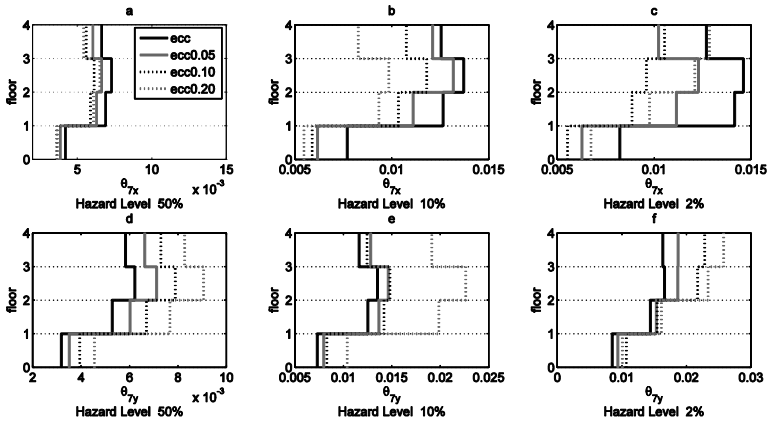

Fig. 23 Test example 4-Column 7 maximum absolute drift values along *x* (a, b, c) and *y* (d, e, f) direction for all floors and hazard levels

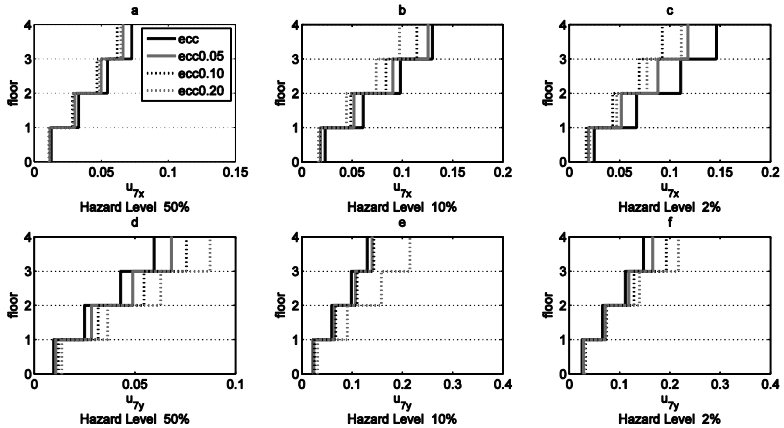

Fig. 24 Test example 4-Column 7 maximum absolute displacement values along *x* (a, b, c) and *y* (d, e, f) direction for all floors and hazard levels

In order to present the variation on the envelopes of the maximum values of the response quantities along the height for all designs, col6 and col7 are selected for demonstration. Both columns are located at the stiff edge along the *x* direction, while column 6 is located at the stiff side and column 7 at the flexible side along the *y* direction. The response quantities are decreased for all stories when the building performs in the elastic region since both columns are located at stiff side along *x* direction, while in the elastoplastic region some response quantities are increased (see Figs. 19 to 24). Along the *y* direction the response quantities of column 6 are decreased proportionally to the increase of eccentricity (5% and 10%), while for column 7 they are increased in both elastic and elastoplastic range.

6. Conclusions

The main objective of the present study is to propose an index which can quantitatively assess the effect of the total induced torsion in mass-irregular building structures. In order to validate and verify the reliability of the proposed *ROT* index, two single-story and two multistory torsionally-stiff buildings are considered. In particular, double eccentric, regular as well as irregular in plan buildings are examined. Nonlinear dynamic analyses are conducted using natural record scaled to three hazard levels.

The proposed index was proved to be a reliable and sufficient measure for assessing the torsional effects of non-symmetric buildings since it was shown that its values follow the trend of base torque, while the rotation of the upper diaphragm was not in agreement with base torque for all the test examples considered. Furthermore, it quantifies the torsional effect in terms of additional induced shear forces at every vertical structural element (in a global way), while it was found to be consistent for all states of response with base torque. Last but not least, it is not required to perform additional analyses in order to draw conclusions regarding the influence of the torsional effect on the structural response.

More specifically from the numerical investigation conducted it can be concluded that:

• For more realistic structural systems with eccentricity, the values of base torque and *ROT* are increased compared to the results obtained for 10/50 and 2/50 hazard levels, while the values of diaphragm rotation are reduced.

• The already observed trend in various studies in the literature, that response quantities are increased at flexible edge and decreased at the stiff edge, has been verified with *ROT* for all regular systems studied, while it was also confirmed for those with horizontal irregularity.

• The proposed index proved to be independent of the state of response since its performance proved to be satisfactory for both elastic and elastoplastic response.

• *ROT* can be calculated easily from the shear forces induced in the structure which can be obtained by routine computations. Thus, it provides practitioner engineers with a useful tool in order to assess the magnitude of influence of torsion on the structural response.

• *ROT* assessment index can be used for improving the final design since reducing *ROT* will lead to reduction of the torsion-induced internal shear forces.

Acknowledgments

The research of C.S. has been co-financed by the European Union (European Social Fund -

ESF) and Greek national funds through the Operational Program "Education and Lifelong Learning" of the National Strategic Reference Framework (NSRF) - Research Funding Program: Heracleitus II. Investing in knowledge society through the European Social Fund. The work of M.P. has been supported by the European Research Council Advanced Grant "MASTER-Mastering the computational challenges in numerical modeling and optimum design of CNT reinforced composites" (ERC-2011-ADG_20110209).

References

Anagnostopoulos, S.A., Alexopoulou, Ch. and Stathopoulos, K.G. (2010), "An answer to an important controversy and the need for caution when using simple models to predict inelastic earthquake response of buildings with torsion", *Earthq. Eng. Struct. Dyn.*, **39**(5), 521-540.

Anagnostopoulos, S.A., Kyrkos, M.T. and Stathopoulos, K.G. (2015), "Earthquake induced torsion in buildings: critical review and state of the art", *Earthq. Struct.*, **8**(2), 305-377.

Bosco, M., Ferrara, G.A.F., Ghersi, A., Marino, E.M. and Rossi, P.P. (2015), "Seismic assessment of existing r.c. framed structures with in-plan irregularity by nonlinear static methods", *Earthq. Struct.*, **8**(2), 401-422.

Bosco, M., Marino, E.M. and Rossi, P.P. (2013), "An analytical method for the evaluation of the in-plan irregularity of non-regularly asymmetric buildings", *Bull. Earthq. Eng.*, **11**(5), 1423-1445.

Chandler, A.M. and Duan, X.N. (1997), "Performance of asymmetric code-designed buildings for serviceability and ultimate limit states", *Earthq. Eng. Struct. Dyn.*, **26**(7), 717-736.

Chandler, A.M., Duan, X.N. and Rutenberg, A. (1996), "Seismic torsional response: assumptions, controversies and research progress", *Eur. Earthq. Eng.*, **10**(1), 37-51.

Cheung, V.W.-T. and Tso, W.K. (1986), "Eccentricity in irregular multistory buildings", *Can. J. Civ. Eng.*, **13**(1), 46-52.

Chopra, A.K. and Goel, R.K. (1991), "Evaluation of torsional provisions in seismic codes", *J. Struct. Eng.*, **117**(12), 3762-3782.

De La Colina, J. (1999), "Effects of torsion factors on simple non-linear systems using fully bidirectional analyses", *Earthq. Eng. Struct. Dyn.*, **28**(7), 691-706.

De La Llera, J.C. and Chopra, A.K. (1995), "A simplified model for analysis and design of asymmetric plan buildings", *Earthq. Eng. Struct. Dyn.*, **24**(4), 573-594.

De La Llera, J.C. and Chopra, A.K. (1995), "Understanding the inelastic seismic behaviour of asymmetric plan buildings", *Earthq. Eng. Struct. Dyn.*, **24**(4), 549-572.

EC8-Eurocode 8 (2004), *Design provisions for earthquake resistance of structures*, European StandardEN1998-1.

Fragiadakis, M. and Papadrakakis, M. (2008), "Modelling, analysis and reliability of seismically excited structures: Computational issues", *Int. J. Comput. Meth.*, **5**(4), 483-511.

Georgoussis, G.K. (2014), "Modified seismic analysis of multistory asymmetric elastic buildings and suggestions for minimizing the rotational response", *Earthq. Struct.*, **7**(1), 39-55.

Humar, J. and Kumar, P. (1998), "A new look at torsion design provisions in seismic building codes", *12th World Conference on Earthquake Engineering*.

Humar, J.L. (1984), "Design for seismic torsional forces", *Can. J. Civ. Eng.*, **11**(2), 150-163.

Jeong, S.-H. and Elnashai, A.S. (2005), "Analytical assessment of an irregular RC frame for full-scale 3D pseudo-dynamic testing part I: Analytical model verification", *J. Earthq. Eng.*, **9**(1), 95-128.

Karimiyan, S., Moghadam, A.S., Karimiyan, M. and Kashan, A.H. (2013), "Seismic collapse propagation in 6-story RC regular and irregular buildings", *Earthq. Struct.*, **5**(6), 753-779.

Kent, D.C. and Park, R. (1971), "Flexural members with confined concrete", *J. Struct. Div.*, **97**(7), 1969-1990.

Kyrkos, M.T. and Anagnostopoulos, S.A. (2011a), "An assessment of code designed, torsionally stiff, asymmetric steel buildings under strong earthquake excitations", *Earthq. Struct.*, **2**(2), 109-126.
Kyrkos, M.T. and Anagnostopoulos, S.A. (2011b), "Improved earthquake resistant design of torsionally stiff asymmetric steel buildings", *Earthq. Struct.*, **2**(2), 127-147.
Kyrkos, T.M. and Anagnostopoulos, A.S. (2013), "Improved earthquake resistant design of eccentric steel buildings", *Soil Dyn. Earthq. Eng.*, **47**, 144-156.
Lagaros, N.D., Papadrakakis, M. and Bakas, N. (2006), "Automatic minimization of the rigidity eccentricity of 3D reinforced concrete buildings", *J. Earthq. Eng.*, **10**(3), 1-32.
Lucchini, A., Monti, G. and Kunnath, S. (2009), "Seismic behavior of single-storey asymmetric-plan buildings under uniaxial excitation", *Earthq. Eng. Struct. Dyn.*, **38**(9), 1053-1070.
Makarios, T. (2008), "Practical calculation of the torsional stiffness radius of multi-storey tall buildings", *Struct. Des. Tall Spec. Build.*, **17**(1), 39-65.
Makarios, T. and Anastassiadis, A. (1998a), "Real and fictitious elastic axes of multi-storey buildings: theory", *Struct. Des. Tall Spec. Build.*, **7**(1), 33-55.
Makarios, T. and Anastassiadis, A. (1998b), "Real and fictitious elastic axes of multi-storey buildings: applications", *Struct. Des. Tall Spec. Build.*, **7**(1), 57-71.
Marino, E.M. and Rossi, P.P. (2004), "Exact evaluation of the location of the optimum torsion axis", *Struct. Des. Tall Spec. Build*, **13**(4), 277-290.
Marušić, D. and Fajfar, P. (2005), "On the inelastic seismic response of asymmetric buildings under bi-axial excitation", *Earthq. Eng. Struct. Dyn.*, **34**(8), 943-963.
McKenna, F. and Fenves, G.L. (2001), *The OpenSees Command Language Manual - Version 1.2*, Pacific Earthquake Engineering Research Centre, University of California, Berkeley.
Myslimaj, B. and Tso, W.K. (2005), "A Design-oriented approach to strength distribution in single-story asymmetric systems with elements having strength dependent stiffness", *Earthq. Spectra*, **21**(1), 197-212.
Myslimaj, B. and Tso, W.K. (2002), "A strength distribution criterion for minimizing torsional response of asymmetric wall-type systems", *Earthq. Eng. Struct. Dyn.*, **31**(1), 99-120.
Palermo, M., Silvestri, S., Gasparini, G. and Trombetti, T. (2013), "Physically-based prediction of the maximum corner displacement magnification of one-storey eccentric systems", *Bull. Earthq. Eng.*, **11**(5), 1467-1491.
Papachristidis, A., Fragiadakis, M. and Papadrakakis, M. (2010), "A 3D fiber beam-column element with shear modeling for the inelastic analysis of steel structures", *Comput. Mech.*, **45**(6), 553-572.
Papazachos, B.C., Papaioannou, Ch.A. and Theodulidis, N.P. (1993), "Regionalization of seismic hazard in Greece based on seismic sources", *Nat. Hazards*, **8**(1), 1-18.
Paulay, T. (1997), "Displacement-based design approach to earthquake induced torsion in ductile buildings", *Eng. Struct.*, **9**(9), 699-707.
Paulay, T. (1998), "Torsional mechanisms in ductile building systems", *Earthq. Eng. Struct. Dyn.*, **27**(10), 1101-1121.
Peruš, I. and Fajfar, P. (2005), "On the inelastic torsional response of single-storey structures under bi-axial excitation", *Earthq. Eng. Struct. Dyn.*, **34**(8), 931-941.
Poole, R.A. (1977), "Analysis for torsion employing provisions of NZRS 4203", *Bull. NZ. Soc. Earthq. Eng.*, **10**(4), 219-225.
Reem, H. and Chopra, A.K. (1987), *Earthquake Response of Torsionally-Coupled Buildings*, Earthquake Engineering Research Centre, College of Engineering, University of California at Berkeley.
Riddel, R. and Vasquez, J. (1984), "Existence of centres of resistance and torsional uncoupling of earthquake response of buildings", *Proceedings of 8thWorld Conference on Earthquake Engineering*, **4**, 187-194.
Rutenberg, A. (2002), "EAEE Task Group (TG) 8: Behaviour of irregular and complex structures-progress since 1998", *Proceedings of the 12th European Conference in Earthquake Engineering*, London.
Scott, B.D., Park, R. and Priestley, M.J.N. (1982), "Stress-Strain behavior of concrete confined by overlapping hoops at low and high strain rates", *ACI J.*, **79**, 13-27.
Smith, B.S. and Vezina, S. (1985), "Evaluation of centers of resistance in multistorey building structures",

Proceedings Of Institution Of Civil Engineers, Part 2, Institution of Civil Engineers, **79**(4), 623-635.
Somerville, P. and Collins, N. (2002), "Ground motion time histories for the Humboldt bay bridge", Pasadena, CA, URS Corporation.
Stathi, Ch.G. (2014), "Optimum design of earthquake resistant structures implementing computational methods", Ph.D. Dissertation, NTUA, Athens, Greece.
Stathopoulos, K.G. and Anagnostopoulos, S.A. (2003), "Inelastic earthquake response of single-story asymmetric buildings: an assessment of simplified shear-beam models", *Earthq. Eng. Struct. Dyn.*, **32**(12), 1813-1831.
Trombetti, T.L. and Conte, J.P. (2005), "New insight into and simplified approach to seismic analysis of torsionally coupled one-story, elastic systems", *J. Sound Vib.*, **286**(1), 265-312.
Tso, W.K. (1990), "Static eccentricity concept for torsional moments estimations", *J. Struct. Eng.*, **116**(5), 1199-1212.

SA